# Topology during Subdivision of Bézier Curves II: Ambient Isotopy

J. Li[a], T. J .Peters [1b], J. A. Roulier[c]

[a] *Department of Mathematics, University of Connecticut, Storrs.*
[b] *Department of Computer Science and Engineering, University of Connecticut, Storrs.*
[c] *Department of Computer Science and Engineering, Univeristy of Connecticut, Storrs.*

**Abstract**

It is of increasing contemporary interest to preserve ambient isotopy during geometric modeling. Bézier curves are pervasive in computer aided geometric design, as one of the fundamental computational representations for geometric modeling. For Bézier curves, subdivision algorithms create control polygons as piecewise linear ($PL$) approximations that converge under Hausdorff distance. A natural question is whether subdivision produces topologically reliable $PL$ approximations. Here we focus upon ambient isotopy and prove that sufficiently many subdivisions produce a control polygon ambient isotopic to the Bézier curve. We also derive closed-form formulas to compute the number of subdivision iterations to ensure ambient isotopic equivalence in the resulting approximation. This work relies upon explicitly constructing homeomorphism and ambient isotopy, which provides more algorithmic efficiency than only showing the existence of these equivalence relations.

*Keywords:* Bézier curve, subdivision, knot, piecewise linear approximation, non-self-intersection, homeomorphism, ambient isotopy.

*2000 MSC:* 57Q37, 57M50, 57Q55, 68R10

[1]This author was partially supported by NSF grants CCF 0429477, CMMI 1053077 and CNS 0923158. All statements here are the responsibility of the author, not of the National Science Foundation.

## 1. Introduction

Ambient isotopy is a stronger notion of equivalence than homeomorphism. Precisely, isotopy is a homotopy with the requirement of a homeomorphism at each value of the time parameter, which is particularly applicable for time varying models. Based on the concurrent result of angular convergence and homeomorphism [15], here we establish the stronger equivalence relation between Bézier curves and the control polygons.

A Bézier curve (Definition 3.1) is characterized by an indexed set of points, which form a $PL$ approximation of the curve, called a control polygon (Definition 3.1). The de Casteljau algorithm [9, 15] is a subdivision algorithm associated to Bézier curves which recursively generate control polygons more closely approximating the curve under Hausdorff distance [24].

There is contemporary interest [1, 2, 18, 22] to preserve topological characteristics such as homeomorphism and ambient isotopy between an initial geometric model and its approximation. In particular, a control polygon ambient isotopic to the Bézier curve is considered having the same embedding in Knot theory. These are fundamental for applications in computer graphics, computer animation and scientific visualization.

However, there may be substantial topological differences between Bézier curves and their control polygons. There is an example showing an unknotted Bézier curve with a knotted control polygon [3, 21]. An example of a knotted Bézier curve with an unknotted control polygon was constructed recently [14].

Although there may be substantial topological differences between a Bézier curve and its initial control polygon, we prove that sufficiently many subdivisions will generate a control polygon that is ambient isotopic (and therefore, necessarily homeomorphic) to the curve. We provide closed-form formulas to compute a sufficient number of subdivisions to achieve this ambient isotopy.

## 2. Related Work

The topological characteristics for a Bézier curve and the control polygon have been studied in the literature. There is an existing proof [26] of homeomorphism under subdivision relied upon the hodograph[2] and did not provide the number of subdivision iterations. A geometrically constructive

[2]The derivative of a Bézier curve is also expressed as a Bézier curve, known as the *hodograph* [9].

proof is established simultaneously, which provides the number of subdivision iterations [15]. Topologically reliable approximation in terms of homeomorphism of composite Bézier curves was also studied by algorithmic techniques that do not completely rely upon de Casteljau algorithm. Instead, that work starts with choosing so called "significant points" [6].

Ambient isotopy for geometric models was obtained by a certain algorithm distinct from subdivision [11]. Recent papers [4, 16] present algorithms to compute the isotopic polygonal approximation for $2D$ algebraic curves. Computational techniques for establishing isotopy and homotopy have been established regarding algorithms for point-cloud data by "distance-like functions" [5]. The input data here is different of a Bézier curve, with the important additional result of the number of subdivision iterations needed to attain an ambient isotopic approximation of the original Bézier curve.

Ambient isotopy under subdivision was previously established [22] for $3D$ Bézier curves of low degree (less than 4), where a crucial unknotting condition was trivial. The results presented here extend the earlier theorem to Bézier curves of arbitrary degrees. The focus on higher degree versions was motivated by applications in molecular simulation where Bézier curve models are created on input of hundreds of thousands of points, with interest in having curves that are at least $C^1$. Preserving that continuity over low degree models on this magnitude of points would be extremely tedious.

Recent progress regarding isotopy under certain convergence criteria has been made [7, 13]. These are nice theorems applicable to Bézier curves. However, they do not necessarily provide formulas to compute the number of subdivision iterations, which is computationally crucial, as Bézier curves are used in many practical areas.

Convergence of the control polygon to a Bézier curve under subdivision in terms of Hausdorff distance is well known [24, 25]. For a space curve, it is known how to construct a "nice" tubular neighborhood, that is, a neighborhood bounded by a nonsingular pipe surface [17]. Based on the convergence in distance, one may obtain a control polygon that fits inside the tubular neighborhood. Pipe surfaces have been studied since the 19th century [20], but the presentation here follows a contemporary source [17]. These contemporary authors [17] provide sufficient conditions for a pipe surface to be nonsingular when its spine curve is regular and $C^1$, as is true for $\mathcal{B}$. These authors perform a thorough analysis and description of the end conditions of open curves. The junction points of $\mathcal{B}$ are merely a special case of that analysis.

## 3. Definitions and Notation

Mathematical definitions, notation and a fundamental supportive theorem are presented in this section. More specialized definitions will follow in appropriate sections. The standard Euclidean norm will be denoted by $||\quad||$.

**Definition 3.1.** *The parameterized* ***Bézier curve****, denoted as $\mathcal{B}(t)$, of degree $n$ with control points $P_m \in \mathbb{R}^3$ is defined by*

$$\mathcal{B}(t) = \sum_{m=0}^{n} B_{m,n}(t) P_m, t \in [0,1],$$

*where $B_{m,n}(t) = \binom{n}{m} t^m (1-t)^{n-m}$ and the $PL$ curve given by the points $\{P_0, P_1, \ldots, P_n\}$ is called its* ***control polygon****. When $P_0 = P_n$, the control polygon is closed. Otherwise when $P_0 \neq P_n$, it is open.*

In order to avoid technical considerations and to simplify the exposition, the class of Bézier curves considered will be restricted to those where the first derivative never vanishes.

**Definition 3.2.** *A differentiable curve is said to be* ***regular*** *if its first derivative never vanishes.*

**Definition 3.3.** *A curve is said to be* ***simple*** *if it is non-self-intersecting.*

The Bézier curve of Definition 3.1 is typically called a *single segment Bézier curve*, while a *composite Bézier curve* is created by joining two or more single segment Bézier curves at their common end points.

**We use $\mathcal{B}$ to denote a simple, regular, $C^1$, composite Bézier curve in $\mathbb{R}^3$, throughout the paper.**

**Definition 3.4.** [24] *Let $X$ and $Y$ be two non-empty subsets of a metric space $(M, d)$. We define their* ***Hausdorff distance*** *$\mu(X, Y)$ by*

$$\mu(X,Y) := \max\{\sup_{x \in X} \inf_{y \in Y} d(x,y), \sup_{y \in Y} \inf_{x \in X} d(x,y)\}.$$

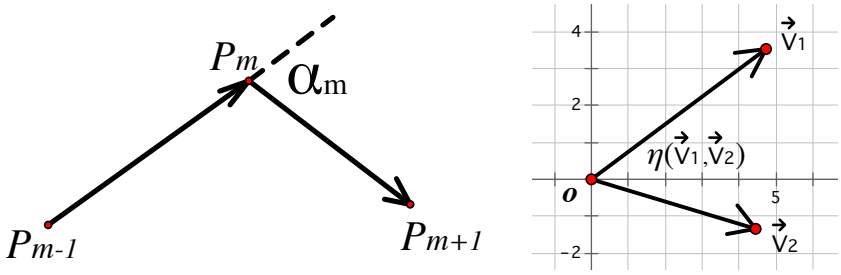


(a) Orientated lines (b) Vectors

Figure 1: An exterior angle

Exterior angles were defined [19] in the context of closed $PL$ curves, but are adapted here for both closed and open $PL$ curves. Exterior angles unify the concept of total curvature for curves that are $PL$ or differentiable.

**Definition 3.5.** *The **exterior angle** between two oriented line segments, denoted as $\overrightarrow{P_{m-1}P_m}$ and $\overrightarrow{P_mP_{m+1}}$, is the angle between the extension of $\overrightarrow{P_{m-1}P_m}$ and $\overrightarrow{P_mP_{m+1}}$, as shown in Figure 1(a). Let the measure of the exterior angle to be $\alpha_m$ satisfying:*

$$0 \leq \alpha_m \leq \pi.$$

*This definition naturally generalizes to any two vectors, $\vec{v}_1$ and $\vec{v}_2$, by joining these vectors at their initial points, while denoting the measure between them as $\eta(\vec{v}_1, \vec{v}_2)$, as indicated in Figure 2(b).*

**Definition 3.6.** *The **curvature** of a $C^2$ curve $C(t)$ parametrized on $[a, b]$ is given by*

$$\kappa(t) = \frac{||C'(t) \times C''(t)||}{||C'(t)||^3}, \quad t \in [a, b]. \tag{1}$$

*Its **total curvature** [8] is the integral: $\int_a^b |\kappa(t)|\, dt$.*

Total curvature can be defined for both $C^2$ and $PL$ curves. In both cases, the total curvature is denoted by $T_\kappa(\cdot)$. The unified terminology is invoked in Fenchel's theorem, which follows and is fundamental to the work presented here.

**Definition 3.7.** [19] *The **total curvature** of a $PL$ curve in $\mathbb{R}^3$ is the sum of the measures of the exterior angles.*

Fenchel's Theorem [8] presented below is applicable both to $PL$ curves and to differentiable curves.

**Theorem 3.1.** [8, Fenchel's Theorem] *The total curvature of any closed curve is at least $2\pi$, with equality holding if and only if the curve is convex.*

Denote a $PL$ curve with vertices $\{P_0, P_1, \cdots, P_n\}$ by $P$, and the uniform parametrization [23] of $P$ over $[0,1]$ by $l(P)_{[0,1]}$. That is:

$$l(P)_{[0,1]}(\frac{j}{n}) = P_j \ for \ j = 0, 1, \cdots, n$$

and $l(P)_{[0,1]}$ interpolates linearly between vertices.

**Definition 3.8.** ***Discrete derivatives*** *[23] are first defined at the parameters $t_j = \frac{j}{n}$, where*

$$l(P)_{[0,1]}(t_j) = P_j$$

*for $j = 0, 1, \cdots, n-1$. Let*

$$P'_j = l'(P)_{[0,1]}(t_j) = \frac{P_{j+1} - P_j}{t_{j+1} - t_j}.$$

*Denote $P' = (P'_0, P'_1, \cdots, P'_{n-1})$. Then define the discrete derivative for $l(P)_{[0,1]}$ as:*

$$l'(P)_{[0,1]} = l(P')_{[0,1]}.$$

Intuitively, the first discrete derivatives are similar to the slopes defined for univariate real-valued functions within an introductory calculus course.

The definition given here is specialized to $\mathbb{R}^n$ as sufficient for the applications intended, but further generalizations are available [10]:

**Definition 3.9.** *Two subspaces of $\mathbb{R}^n$, denoted by $X$ and $Y$, are said to be* ***ambient isotopic*** *if there exists a continuous map $H : \mathbb{R}^n \times [0,1] \to \mathbb{R}^n$ satisfying:*

*(1) $H(\cdot, 0)$ is the identity,*

*(2) $H(X, 1) = Y$, and*

*(3) $\forall t \in [0,1]$, $H(\cdot, t) : \mathbb{R}^n \to \mathbb{R}^n$ is a homeomorphism.*

*The map $H$ is an ambient isotopy between $X$ and $Y$.*

**Definition 3.10.** *The* ***pipe surface*** *of radius $r$ of a parameterized curve $\boldsymbol{c}(t)$, where $t \in [0,1]$ is given by*

$$\boldsymbol{p}(t,\theta) = \boldsymbol{c}(t) + r[cos(\theta)\ \boldsymbol{n}(t) + sin(\theta)\ \boldsymbol{b}(t)],$$

*where $\theta \in [0, 2\pi]$ and $\boldsymbol{n}(t)$ and $\boldsymbol{b}(t)$ are, respectively, the normal and binormal vectors at the point $\boldsymbol{c}(t)$, as given by the Frenet-Serret trihedron. The curve $\boldsymbol{c}$ is called a spine curve.*

**Remark 3.1.** *The paper [17] provides the computation of the radius $r$ only for rational spline curves. However, the method of computing $r$ is similar for other compact, regular, $C^2$, and simple curves, that is, taking the minimum of $1/\kappa_{max}$, $d_{min}$, and $r_{end}$, where $\kappa_{max}$ is the maximum of the curvatures, $d_{min}$ is the minimum separation distance, and $r_{end}$ is the maximal radius around the end points that does not yield self-intersections.*

## 4. Construction of Homeomorphisms

Homeomorphism is a necessary condition for ambient isotopy. The existence of a homeomorphism between $\mathcal{B}$ and the control polygon is shown in the companion paper [15]. However, constructing the ambient isotopy here relies upon explicitly constructing a homeomorphism. The explicit construction provides more algorithmic efficiency than only showing the existence of these equivalence relations[3].

We shall find two criteria (*Hypotheses 1, 2*) to ensure the ambient isotopy between a $PL$ curve and a $C^2$ curve. We then show that these criteria can be achieved for a Bézier curve by subdivision. Based on this, we shall construct an ambient isotopy between a Bézier curve and the control polygon in Section 5.

Let $L$ be an open, compact, and simple $PL$ parametric curve and $C$ to be an open, compact, simple, regular, and $C^2$ polynomial curve of degree $n$ in $\mathbb{R}^3$. Let $L(t) : [0,1] \to \mathbb{R}^3$ and $C(t) : [0,1] \to \mathbb{R}^3$ be the corresponding

[3]There is an alternative proof of the ambient isotopy [12], which requires the convex hulls of sub-control polygons to be contained in the tubular neighborhood determined by a pipe surface. This containment makes the proof easier, but likely needs too many subdivision iterations and produces too many $PL$ segments. However it is valuable for theoretical insight.

parameterizations of $L$ and $C$. We consider the homeomorphism between $L$ and $C$, when $L(0) = C(0),\ L(1) = C(1)$, that is, $L \cup C$ forms a closed curve[4].

Since $C$ is a compact, simple, regular, and $C^2$ curve, there exists a nonsingular pipe surface (Remark 3.1) of radius $r$. Denote the disc of radius $r$ centered at $C(t)$ and normal to $C$ as $D_r(t)$. Let a **pipe section** to be $\Gamma = \bigcup_{t\in[0,1]} D_r(t)$. Denote the interior as $\text{int}(\Gamma)$, and the boundary as $\partial\Gamma$. Note that the boundary $\partial\Gamma$ consists of the nonsingular pipe surface (Definition 3.10) and the end discs $D_r(0)$ and $D_r(1)$.

**Definition 4.1.** *Define* $\theta(t) : [0,1] \to [0,\pi]$ *by*

$$\theta(t) = \eta(C'(t), L'(t)),$$

*where the function* $\eta(\cdot,\cdot)$ *was previously given in Definition 3.5.*

**The following *Hypotheses 1* and *2* will play a central role to the following lemmas, and in establishing the homeomorphism.**

*Hypothesis 1:* $L \setminus \{L(0), L(1)\} \subset \text{int}(\Gamma)$; and
*Hypothesis 2:* $T_\kappa(L) + \max_{t\in[0,1]} \theta(t) < \frac{\pi}{2}$,

where $\Gamma$ is the pipe section of $C$ and $T_\kappa(L)$ denotes the total curvature of $L$.

**Lemma 4.1.** *Suppose $L$ is a sub-control polygon and $C$ is the corresponding Bézier sub-curve. Then Hypotheses 1* and *2 can be achieved by subdivision.*

**Proof:** By the convergence in Hausdorff distance under subdivision, sufficiently many subdivision iterations will produce a control polygon that fits inside a nonsingular pipe surface. Furthermore, by the Angular Convergence [15, Theorem 4.1] and the lemma [15, Lemma 5.2] in the companion paper, possibly more subdivisions will ensure that each sub-control polygon lies in the corresponding nonsingular pipe section, which is the *Hypothesis 1.* Denote the number of subdivision iterations to achieve this by $\iota_1$.

By the Angular Convergence [15, Theorem 4.1], $T_\kappa(L)$ converges to 0 under subdivision. Because the discrete derivative of the control polygon converges to the derivative of the Bézier curve [23] under subdivision, $\theta(t)$

[4]Any pairwise disjoint simple open curves are trivially ambient isotopic.

converges to 0 for each $t \in [0,1]$. So *Hypothesis 2* will be achieved by sufficiently many subdivision iterations, say $\iota_2$. (The Details to find $\iota_1$ and $\iota_2$ are in Section 6.) $\square$

**Remark 4.1.** *When we consider the number of subdivision iterations later, we shall show that the sufficient number of subdivisions for Hypothesis 2 is at most one more than that for a weaker condition $T_\kappa(L) < \frac{\pi}{2}$. (Remark 6.1 in Section 6)*

**Remark 4.2.** *To obtain some intuition for these hypotheses, restrict our attention to a Bézier curve. Consider $L$ to be a sub-control polygon and $C$ to be the corresponding sub-curve. Hypothesis 1 will ensure that $L$ lies inside a nonsingular pipe section, while Hypothesis 2 will ensure a local homeomorphism between $L$ and $C$. In particular, Hypotheses 1* and *2 will be sufficient for us to establish the one-to-one correspondence using normal discs of $C$.*

***Hypotheses 1* and *2* are assumed in the rest of the section.**
Define a function $\tilde{L}(t) : [0,1] \to L$ by letting

$$\tilde{L}(t) = D_r(t) \cap L, \tag{2}$$

where $D_r(t)$ is the normal disc of $C$ at $t$.

Define a map $h : C \to L$ for each $p \in C$ by setting

$$h(p) = \tilde{L}(C^{-1}(p)). \tag{3}$$

We shall show that $h$ is a homeomorphism. The subtlety here is to demonstrate the one-to-one correspondence by showing each normal disc of $C$ intersects $L$ at a single point (which will be the main goal of the following), and intersects $C$ at a single point (which will be easy), under the assumption of *Hypotheses 1* and *2*.

*4.1. Outline of the Proof*

For an arbitrary $t_0 \in [0,1]$, the associated normal disc is denoted as $D_r(t_0)$. Following is the sketch of proving that $D_r(t_0)$ intersects $L$ at a single point. (See Figure 2.)

1. *The essential initial steps are to select a non-vertex point of $L$, denoted as $w$, a plane, denoted as $\Omega$, and an angle, denoted as $\theta(t_0)$:*

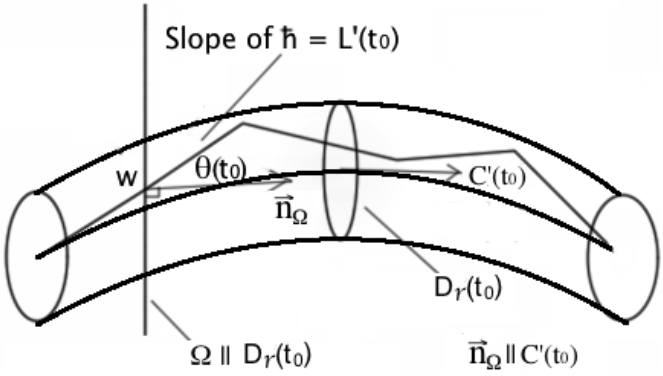


Figure 2: Each normal disc intersects $L$ at a single point

(a) Define $w$ and $\Omega$: Pick a line segment of $L$ whose slope is equal to $L'(t_0)$, denoted as $\hbar$. Choose an interior point of $\hbar$, denoted as $w$. Let $\Omega$ be the plane that contains $w$ and is parallel to $D_r(t_0)$. (We use $w$ to define two sub-curves of $L$, a 'left' sub-curve which terminates at $w$, denoted as $L_l$, and a 'right' sub-curve which begins at $w$, denoted as $L_r$.)

(b) Consider $\eta(C'(t_0), L'(t_0)) = \theta(t_0)$ (Definition 4.1). Since $\Omega$ is parallel to $D_r(t_0)$, a normal vector of $\Omega$, denoted by $\vec{n}_\Omega$ has the same direction as $C'(t_0)$ and $\eta(\vec{n}_\Omega, \hbar) = \eta(C'(t_0), L'(t_0)) = \theta(t_0)$.

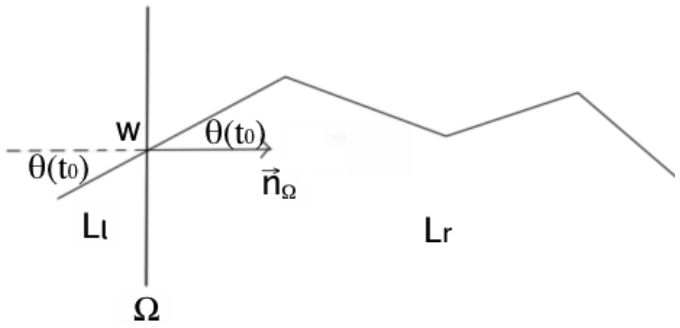


Figure 3: Similar angles $\theta(t_0)$

*Remark:* Since $\eta(\vec{n}_\Omega, \hbar) = \theta(t_0)$, *Hypothesis 2* implies that $T_\kappa(L)+\eta(\vec{n}_\Omega, \hbar) = T_\kappa(L)+\theta(t_0) < \frac{\pi}{2}$. Since $w$ is an interior point of $\hbar$, the angle determined by $\Omega$ and $L_l$, and the angle determined by $\Omega$ and $L_r$, have the same measure $\theta(t_0)$,

as shown in Figure 3. So we obtain the similar inequalities $T_\kappa(L_l)+\theta(t_0) < \frac{\pi}{2}$ and $T_\kappa(L_r) + \theta(t_0) < \frac{\pi}{2}$, which will be crucial.

2. Prove, by *Hypothesis 2*, that $\Omega \cap L_r = w$ . Similarly, show that $\Omega \cap L_l = w$. So $\Omega \cap L = w$. (Lemma 4.3)
3. Prove that any plane parallel to $\Omega$ intersects $L$ at no more than a single point. (Lemma 4.4)
4. Since $D_r(t_0) \parallel \Omega$, it will follow that $D_r(t_0)$ intersects $L$ no more than a single point. Show, using *Hypothesis 1*, that $D_r(t_0)$ must intersect $L$, and hence $D_r(t_0) \cap L$ is a single point. (Lemma 4.5)

*4.2. Preliminary Lemmas for Homeomorphisms*

In order to work with total curvatures of $PL$ curves, an extension of the spherical triangle inequality [27], given in Lemma 4.2, will be useful, similar to previous usage by Milnor [19].

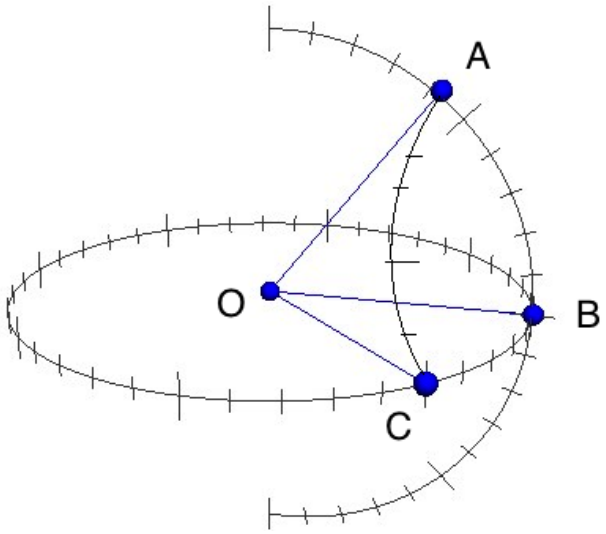


Figure 4: Spherical triangle $\triangle ABC$

**Spherical triangle inequalities:** Consider Figure 4, and the three angles $\angle AOB$, $\angle BOC$, and $\angle AOC$, formed by three unit vectors $\overrightarrow{OA}$, $\overrightarrow{OB}$, and $\overrightarrow{OC}$. (Note the common end point $O$. When we consider angles between vectors that do not share such a common end point, we move the vectors to form a common end point.) Denote the arc length of the curve from $A$ to $B$

as $\ell(\widehat{AB})$, and similarly for that from $B$ to $C$ as $\ell(\widehat{BC})$ and that from $A$ to $C$ as $\ell(\widehat{AC})$. The triangle inequality, $\ell(\widehat{AB}) \leq \ell(\widehat{BC}) + \ell(\widehat{AC})$, of the spherical triangle $\triangle ABC$ provides that

$$\angle AOB \leq \angle BOC + \angle AOC. \tag{4}$$

**Lemma 4.2.** *Suppose that $\vec{v}_1, \vec{v}_2, \ldots, \vec{v}_m$, where $m \in \{3, 4, \ldots\}$, are nonzero vectors, then*

$$\eta(\vec{v}_1, \vec{v}_m) \leq \eta(\vec{v}_1, \vec{v}_2) + \eta(\vec{v}_2, \vec{v}_3), + \ldots, + \eta(\vec{v}_{m-1}, \vec{v}_m). \tag{5}$$

**Proof:** The proof follows easily from Inequality 4. □

Now, we adopt the notation shown in Figure 2 and formalize the proof outlined in Section 4.1. We assume that the sub-curve on the right hand side of $\Omega$ in Figure 3 is $L_r$, and the other one is $L_l$, where we denote the set of ordered vertices of $L_r$ as

$$\{v_0, v_1, \ldots, v_n\},$$

with $v_0 = w$.

By Definition 4.1, we have $\theta(t_0) \leq \max_{t\in[0,1]} \theta(t)$. It is trivially true that $T_\kappa(L_r) \leq T_\kappa(L)$, so that with *Hypothesis 2:* $T_\kappa(L) + \max_{t\in[0,1]} \theta(t) < \frac{\pi}{2}$, we have

$$T_\kappa(L_r) + \theta(t_0) \leq T_\kappa(L) + \max_{t\in[0,1]} \theta(t) < \frac{\pi}{2}. \tag{6}$$

The statement and proof of Lemma 4.3 depend upon the point $w$ chosen in Step 1 of the Outline presented in Section 4.1. There, the point $w$ was defined as an *interior point* of a line segment $\hbar$ of $L$, so that $w$ is precluded from being a vertex of the original PL curve $L$.

**Lemma 4.3.** *The plane $\Omega$ intersects $L$ only at the single point $w$.*

**Proof:** Here we prove $\Omega \cap L_r = w$. A similar argument will show $\Omega \cap L_l = w$.

The oriented initial line segment of $L_r$ is $\overrightarrow{wv_1}$ which lies on $\hbar$. So

$$\eta(\vec{n}_\Omega, \overrightarrow{wv_1}) = \eta(\vec{n}_\Omega, \hbar) = \theta(t_0) < \frac{\pi}{2}.$$

For a proof by contradiction, assume that $\Omega$ intersects $L_r$ at some point $u$ other than $w$. The possibility that $\overrightarrow{wv_1} \subset \Omega$ is precluded by $\theta(t_0) < \pi/2$, so the plane $\Omega$ intersects $\overrightarrow{wv_1}$ only at $w$. So $u \notin \overrightarrow{wv_1}$.

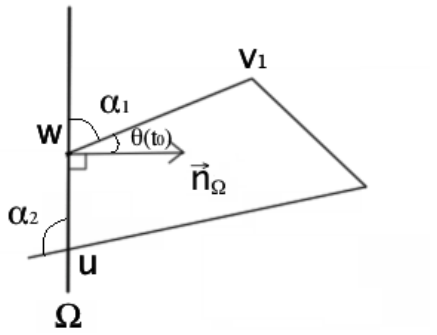


Figure 5: The intersection $u$ generates a closed $PL$ curve

Denote the sub-curve of $L_r$ from $w$ to $u$ as $L(wu)$. Then, since $u \notin \overrightarrow{wv_1}$, the union, $L(wu) \cup \overrightarrow{uw}$, forms a closed $PL$ curve, as Figure 5 shows. By Fenchel's theorem we have

$$T_\kappa(L(wu) \cup \overrightarrow{uw}) \geq 2\pi. \tag{7}$$

Denote the exterior angle of the $PL$ curve $L(wu) \cup \overrightarrow{uw}$ at $w$ as $\alpha_1$ (Figure 5), that is,

$$\alpha_1 = \eta(\overrightarrow{uw}, \overrightarrow{wv_1}).$$

By Inequality 4,

$$\alpha_1 = \eta(\overrightarrow{uw}, \overrightarrow{wv_1}) \leq \eta(\overrightarrow{uw}, \vec{n}_\Omega) + \eta(\vec{n}_\Omega, \overrightarrow{wv_1}).$$

Since $\overrightarrow{uw} \subset \Omega$, we have that $\eta(\overrightarrow{uw}, \vec{n}_\Omega) = \frac{\pi}{2}$. Note also that $\eta(\vec{n}_\Omega, \overrightarrow{wv_1}) = \theta(t_0)$. So

$$\alpha_1 \leq \frac{\pi}{2} + \theta(t_0).$$

Denote the exterior angle of the $PL$ curve $L(wu) \cup \overrightarrow{uw}$ at $u$ as $\alpha_2$. By the definition of exterior angles, we have $\alpha_2 \leq \pi$, so that

$$T_\kappa(L(wu) \cup \overrightarrow{uw}) = \alpha_1 + T_\kappa(L(wu)) + \alpha_2 \leq \frac{\pi}{2} + \theta(t_0) + T_\kappa(L(wu)) + \pi.$$

It follows from Inequality 7 that

$$\frac{\pi}{2} + \theta(t_0) + T_\kappa(L(wu)) + \pi \geq 2\pi,$$

so

$$T_\kappa(L(wu)) + \theta(t_0) \geq \frac{\pi}{2}. \tag{8}$$

By $L(wu) \subset L_r$, we have

$$T_\kappa(L_r) + \theta(t_0) \geq T_\kappa(L(wu)) + \theta(t_0) \geq \frac{\pi}{2}.$$

But this contradicts Inequality 6. □

**Lemma 4.4.** *Any plane parallel to $\Omega$ intersects $L$ at no more than a single point.*

**Proof:** Suppose $\tilde{\Omega}$ is a plane parallel to $\Omega$. If $\tilde{\Omega} \cap L = \emptyset$, then we are done, so we assume that $\tilde{\Omega} \cap L \neq \emptyset$. If $\tilde{\Omega} = \Omega$, then Lemma 4.3 applies, so we also assume that $\tilde{\Omega} \neq \Omega$, implying that $w \notin \tilde{\Omega}$.

Consider two closed half-spaces $\mathbb{H}_l$ and $\mathbb{H}_r$ such that $\mathbb{H}_l \cup \mathbb{H}_r = \mathbb{R}^3$ and $\mathbb{H}_l \cap \mathbb{H}_r = \Omega$. Since $\Omega \cap L_l = \Omega \cap L_r = w$ and $L = L_l \cup L_r$ is simple, we can assume that $L_l \subset \mathbb{H}_l$ and $L_r \subset \mathbb{H}_r$.

Suppose without loss of generality that $\tilde{\Omega} \subset H_r$, as shown in Figure 6. Then since $L_l \subset \mathbb{H}_l$ and $\mathbb{H}_l \cap \mathbb{H}_r = \Omega \neq \tilde{\Omega}$, we have $\tilde{\Omega} \cap L_l = \emptyset$. Since we assumed $\tilde{\Omega} \cap L \neq \emptyset$, it follows that $\tilde{\Omega} \cap L_r \neq \emptyset$. Now, it suffices to show that $\tilde{\Omega} \cap L_r$ is a single point.

Since $L_r$ is compact and oriented, let $\tilde{w}$ denote the first point of $L_r$, at which $\tilde{\Omega}$ intersects $L_r$. Since $\tilde{\Omega} \parallel \Omega$ and $\tilde{\Omega} \neq \Omega$, we have $\tilde{w} \neq w$. We shall show that $\tilde{\Omega} \cap L_r = \tilde{w}$.

Denote the sub-curve of $L_r$ from its initial point $v_0$ to $\tilde{w}$ as $K_1$, and the sub-curve from $\tilde{w}$ to its end point $v_n$ as $K_2$, as shown in Figure 6. Since $\tilde{w}$ is the first intersection point of $\tilde{\Omega} \cap L_r$, but $K_1$ ends in $\tilde{w}$, then it is clear that $\tilde{\Omega} \cap K_1$ contains only $\tilde{w}$. Then in order to show $\tilde{\Omega} \cap L_r = \tilde{w}$, it suffices to show that $\tilde{\Omega} \cap K_2 = \tilde{w}$.

If $\tilde{w} = v_n$, then it is the degenerate case: $K_2 = \tilde{w}$, and we are done. Otherwise, there is a vertex $v_k$ for some $k \in \{1, \ldots, n\}$ such that $\overrightarrow{\tilde{w}v_k}$ is the non-degenerate initial segment of $K_2$, where $\tilde{w} \neq v_k$. Now we shall establish the inequality:

$$T_\kappa(K_2) + \eta(\vec{n}_\Omega, \overrightarrow{\tilde{w}v_k}) < \frac{\pi}{2},$$

to guarantee a single point of intersection, similar to arguments previously given in Lemma 4.3. To this end, we use Inequality 4 to note that

$$\eta(\vec{n}_\Omega, \overrightarrow{\tilde{w}v_k}) \leq \eta(\vec{n}_\Omega, \overrightarrow{v_0v_1}) + \eta(\overrightarrow{v_0v_1}, \overrightarrow{\tilde{w}v_k}) = \theta(t_0) + \eta(\overrightarrow{v_0v_1}, \overrightarrow{\tilde{w}v_k}). \tag{9}$$

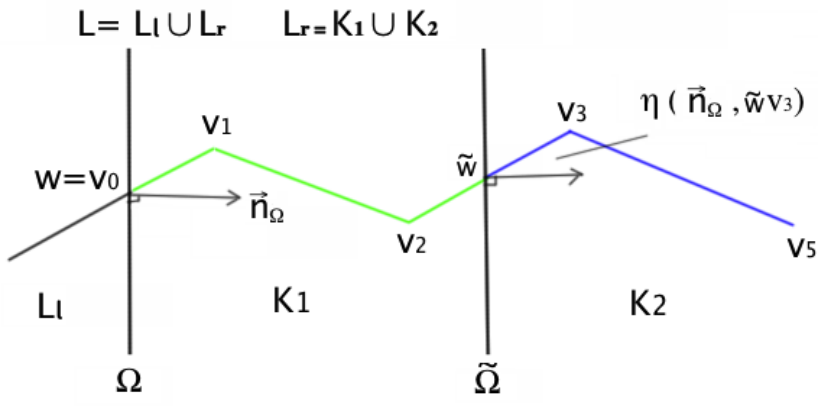


Figure 6: A parallel plane intersecting $L$

The proof will be completed if we can show that

$$T_\kappa(K_2) + \theta(t_0) + \eta(\overrightarrow{v_0v_1}, \overrightarrow{\tilde{w}v_k}) < \frac{\pi}{2}. \tag{10}$$

**Case1:** The intersection $\tilde{w}$ is not a vertex, that is, $\tilde{w} \neq v_{k-1}$. Then $\tilde{w}$ is an interior point of $\overrightarrow{v_{k-1}v_k}$, and hence $T_\kappa(K_1) = \eta(\overrightarrow{v_0v_1}, \overrightarrow{v_1v_2}) + \ldots + \eta(\overrightarrow{v_{k-2}v_{k-1}}, \overrightarrow{v_{k-1}\tilde{w}})$, and $\eta(\overrightarrow{v_{k-1}\tilde{w}}, \overrightarrow{\tilde{w}v_k}) = 0$. By Lemma 4.2,

$$\eta(\overrightarrow{v_0v_1}, \overrightarrow{\tilde{w}v_k}) \leq \eta(\overrightarrow{v_0v_1}, \overrightarrow{v_1v_2}) + \ldots + \eta(\overrightarrow{v_{k-2}v_{k-1}}, \overrightarrow{v_{k-1}\tilde{w}}) + \eta(\overrightarrow{v_{k-1}\tilde{w}}, \overrightarrow{\tilde{w}v_k}) = T_\kappa(K_1).$$

So

$$T_\kappa(K_2) + \theta(t_0) + \eta(\overrightarrow{v_0v_1}, \overrightarrow{\tilde{w}v_k}) \leq T_\kappa(K_2) + \theta(t_0) + T_\kappa(K_1).$$

We also have

$$T_\kappa(L_r) = T_\kappa(K_1) + \eta(\overrightarrow{v_{k-1}\tilde{w}}, \overrightarrow{\tilde{w}v_k}) + T_\kappa(K_2) = T_\kappa(K_1) + T_\kappa(K_2),$$

(since $\eta(\overrightarrow{v_{k-1}\tilde{w}}, \overrightarrow{\tilde{w}v_k}) = 0$), so that

$$T_\kappa(K_2) + \theta(t_0) + \eta(\overrightarrow{v_0v_1}, \overrightarrow{\tilde{w}v_k}) \leq T_\kappa(L_r) + \theta(t_0),$$

which is less than $\frac{\pi}{2}$, by Inequality 6.

**Case2:** The intersection $\tilde{w}$ is a vertex, that is, $\tilde{w} = v_{k-1}$, then $T_\kappa(K_1) = \eta(\overrightarrow{v_0v_1}, \overrightarrow{v_1v_2}) + \ldots + \eta(\overrightarrow{v_{k-3}v_{k-2}}, \overrightarrow{v_{k-2}\tilde{w}})$. By Lemma 4.2,

$$\begin{aligned}
&\eta(\overrightarrow{v_0v_1}, \overrightarrow{\tilde{w}v_k}) \\
&\leq \eta(\overrightarrow{v_0v_1}, \overrightarrow{v_1v_2}) + \ldots + \eta(\overrightarrow{v_{k-3}v_{k-2}}, \overrightarrow{v_{k-2}\tilde{w}}) + \eta(\overrightarrow{v_{k-2}\tilde{w}}, \overrightarrow{\tilde{w}v_k}) \\
&\leq T_\kappa(K_1) + \eta(\overrightarrow{v_{k-2}\tilde{w}}, \overrightarrow{\tilde{w}v_k}).
\end{aligned}$$

So

$$T_\kappa(K_2) + \theta(t_0) + \eta(\overrightarrow{v_0v_1}, \overrightarrow{\tilde{w}v_k}) \leq T_\kappa(K_2) + \theta(t_0) + T_\kappa(K_1) + \eta(\overrightarrow{v_{k-2}\tilde{w}}, \overrightarrow{\tilde{w}v_k}).$$

But by the definition of the total curvature for a $PL$ curve,

$$T_\kappa(K_2) + T_\kappa(K_1) + \eta(\overrightarrow{v_{k-2}\tilde{w}}, \overrightarrow{\tilde{w}v_k}) = T_\kappa(L_r).$$

So

$$T_\kappa(K_2) + \theta(t_0) + \eta(\overrightarrow{v_0v_1}, \overrightarrow{\tilde{w}v_k}) \leq T_\kappa(L_r) + \theta(t_0),$$

which is less than $\frac{\pi}{2}$, by Inequality 6.

So Inequality 10 holds, which is an inequality analogous to Inequality 6. If in the proof of Lemma 4.3, we change $\Omega$ to $\tilde{\Omega}$, $L_r$ to $K_2$ and $\theta(t_0)$ to $\eta(\vec{n}_\Omega, \overrightarrow{\tilde{w}v_k})$, then a similar proof of Lemma 4.3 will show that $\tilde{\Omega} \cap K_2 = \tilde{w}$. This completes the proof. □

**Lemma 4.5.** *For an arbitrary $t_0 \in [0, 1]$, the disc $D_r(t_0)$ intersects $C$ at a unique point, and also intersects $L$ at a unique point.*

**Proof:** First, we have $C(t_0) \in D_r(t_0) \cap C$. If there is an additional point, say $C(t_1) \in D_r(t_0) \cap C$ where $t_1 \neq t_0$, then we have that $C(t_1) \neq C(t_0)$ because $C$ is simple, and hence $D(t_1) \neq D(t_0)$. Since also $C(t_1) \in D_r(t_1)$, we have that $C(t_1) \in D_r(t_0) \cap D_r(t_1)$. But this contradicts the non-self-intersection of $\Gamma$. So $D_r(t_0) \cap C$ must be a unique point.

Now, we show that $D_r(t_0) \cap L \neq \emptyset$. If $t_0 = 0$ or $t_0 = 1$, then since $L(0) \in D_r(0)$ and $L(1) \in D_r(1)$, we have that $D_r(t_0) \cap L \neq \emptyset$.

Otherwise if $t_0 \in (0, 1)$, then assume to the contrary that $D_r(t_0) \cap L = \emptyset$. Since $L \subset \Gamma$ by *Hypothesis 1*, the contrary assumption implies that $L \subset \Gamma \setminus D_r(t_0)$. Because $C$ is an open curve, we have that $D_r(0) \neq D_r(1)$. So

$\Gamma \setminus D_r(t_0)$ consists of two disconnected components, but this implies that $L$ is disconnected, which is a contradiction. So

$$D_r(t_0) \cap L \neq \emptyset. \tag{11}$$

Since $D_r(t_0) \parallel \Omega$ (as discussed in Section 4.1), Lemma 4.4 implies that the plane containing $D_r(t_0)$ intersects $L$ at no more than a single point, which, of course, further implies that $D_r(t_0)$ intersects $L$ at no more than a single point. This plus Inequality 11 shows that $D_r(t_0) \cap L$ is a single point.

If $D_r(t_0) \cap L = D_r(t_1) \cap L$ for some $t_1 \neq t_0$, then $D_r(t_0)$ and $D_r(t_1)$ intersect, which contradicts the non-self-intersection of $\Gamma$. So there is an one-to-one correspondence between the parameter $t$ and the point $D_r(t) \cap L$ for $t \in [0, 1]$, which shows the uniqueness. □

**Lemma 4.6.** *The map $\tilde{L}(t)$ given by Equation 2 is well defined, one-to-one and onto.*

**Proof:** It is well defined by Lemma 4.5. Suppose $\tilde{L}(t_1) = \tilde{L}(t_2)$, then $D_r(t_1) \cap L = D_r(t_2) \cap L$ which is not empty by Lemma 4.5. So $D_r(t_1) \cap D_r(t_2) \neq \emptyset$. Since $\Gamma$ is nonsingular, it follows that $D_r(t_1) = D_r(t_2)$. Since $C$ is simple, if $D_r(t_1) = D_r(t_2)$, then $t_1 = t_2$. Thus $\tilde{L}$ is one-to-one. Since $L \subset \Gamma$, each point of $L$ is contained in some disc $D_r(t)$. So $\tilde{L}$ is onto. □

**Lemma 4.7.** *The map $\tilde{L}(t)$ given by Equation 2 is continuous.*

**Proof:** Let $\Gamma_{t_1 t_2}$ be the portion[5] of $\Gamma$ corresponding to $[t_1, t_2]$, that is

$$\Gamma_{t_1 t_2} = \bigcup_{t \in [t_1, t_2]} D_r(t).$$

Suppose that $s \in [0, 1]$ is an arbitrary parameter. Then by Lemma 4.6, there is a unique point $q \in L$ such that $q = \tilde{L}(s) = D_r(s) \cap L$. We shall prove the continuity of $\tilde{L}(t)$ at $s$ by the definition, that is, for $\forall \epsilon > 0$, there exists a $\delta > 0$ such that $|t - s| < \delta$ implies $||\tilde{L}(t) - \tilde{L}(s)|| < \epsilon$.

Note that $D_r(s)$ divides $\Gamma$ into $\Gamma_{0s}$ and $\Gamma_{s1}$. Since $C$ is an open curve, it follows that $D_r(0) \neq D_r(1)$, and that $\Gamma_{0s}$ and $\Gamma_{s1}$ intersect at only $D_r(s)$. By Lemma 4.5, $D_r(s) \cap L$ is a single point, so $L$ is divided by $D_r(s)$ into two

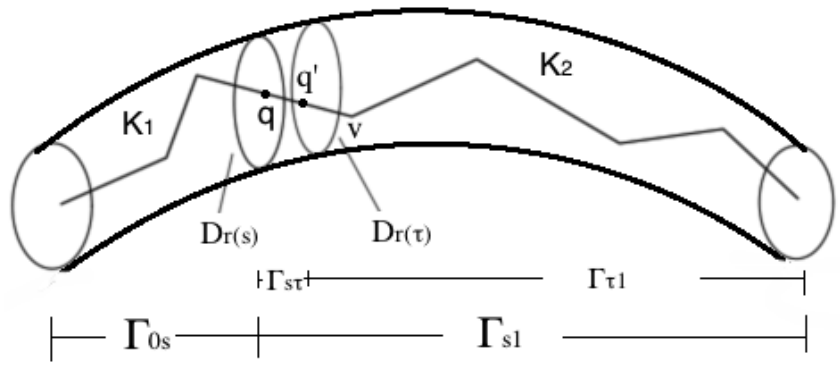


Figure 7: If $|s-\tau| < \delta$, then $||q-q'|| < \epsilon$

sub-curves, denoted as $K_1$ and $K_2$, that is $K_1 \subset \Gamma_{0s}$ and $K_2 \subset \Gamma_{s1}$, as shown in Figure 7.

**Case1:** The parameter $s$ is such that $s \neq 0$ and $s \neq 1$. Consider $\Gamma_{s1}$ first. Since $K_2$ is oriented, we can let $v$ be the first vertex of $K_2$ that is nearest (in distance along $K_2$) to $q$. For any $0 < \epsilon < ||\overline{qv}||$, let $q' \in \overline{qv}$ such that $||\overline{qq'}|| = \epsilon$. By Lemma 4.6, $q' = \tilde{L}(\tau) = D_r(\tau) \cap L$ for some $\tau \in (s, 1]$.

First, note $\overline{qq'} \cap \text{int}\Gamma_{s\tau} \neq \emptyset$. To verify this, observe $\overline{qq'} \subset \overline{qv} \subset K_2 \subset \Gamma_{s1}$ and $\Gamma_{s1} = \Gamma_{s\tau} \cup \Gamma_{\tau 1}$, so $\overline{qq'} \subset \Gamma_{s\tau} \cup \Gamma_{\tau 1}$. If $\overline{qq'} \cap \text{int}\Gamma_{s\tau} = \emptyset$, then the segment $\overline{qq'}$ is contained in $D_r(s) \cup \Gamma_{\tau 1}$ which is disconnected. This implies $\overline{qq'}$ is disconnected, which is a contradiction.

Secondly, note that the subset $\Gamma_{s\tau}$ of a nonsingular pipe section is connected (since $C$ is $C^1$), and $\overline{qq'}$ is a line segment jointing the end discs of $\Gamma_{s\tau}$, and has intersections with interior of $\Gamma_{s\tau}$. This geometry implies that

$$\overline{qq'} \subset \Gamma_{s\tau}. \tag{12}$$

Let $\delta = \tau - s$. For an arbitrary $t \in (s, s+\delta) = (s, \tau)$, Inclusion 12 implies that $\tilde{L}(t) = D_r(t) \cap \overline{qq'}$. Since neither $\tilde{L}(t) \neq q$ or $\tilde{L}(t) \neq q'$, it follows that $\tilde{L}(t) \in \text{int}(\overline{qq'})$. So

$$||\tilde{L}(t) - \tilde{L}(s)|| < ||\overline{qq'}|| = \epsilon.$$

This shows the right-continuity. We similarly consider the $\Gamma_{0s}$ and obtain the left-continuity.

[5] If $t_1 = t_2$, then $\Gamma_{t_1 t_2}$ is a single disc.

**Case2:** The parameter $s$ is such that $s = 0$ or $s = 1$. We similarly obtain the right-continuity if $s = 0$, or the left-continuity if $s = 1$. □

**Theorem 4.1.** *If $L$ and $C$ satisfy Hypotheses 1* and *2, then the map $h$ defined by Equation 3 is a homeomorphism.*

**Proof:** By Lemma 4.6, $\tilde{L}(t)$ is one-to-one and onto. By Lemma 4.7, $\tilde{L}(t)$ is continuous. Since $\tilde{L}$ is defined on a compact domain, it is a homeomorphism.

Note that $C$ is simple and open, so $C(t)$ is one-to-one, and it is obviously onto. The map $C(t)$ is also continuous and defined on a compact domain, so $C(t)$ a homeomorphism. Since $h$ is a composition of $C^{-1}$ and $\tilde{L}$, $h$ is a homeomorphism. □

**Remark 4.3.** *A very natural way to define a homeomorphism between simple curves $C$ and $L$ would be by $f(p) = L(C^{-1}(p))$. An easy method to extend $f$ to a homotopy is the straight-line homotopy. However, we were not able to establish that a straight-line homotopy based upon $f$ would also be an isotopy, where it would be necessary to show that each pair of line segments generated is disjoint. Our definition of $h$ in Equation 3 was strategically chosen so that this isotopy criterion is easily established, since the normal discs are already pairwise disjoint.*

## 5. Construction of ambient isotopies

Note that $L$ and $C$ fit inside a nonsingular pipe section (Remark 3.1) $\Gamma$ of $C$. For a similar problem, an explicit construction has appeared [18, Section 4.4] [11]. The proof of Lemma 5.3, below, is a simpler version of a previous proof [11, Corollary 4]. The construction here relies upon some basic properties of convex sets, which are repeated here. For clarity, the complete proof of Lemma 5.3 is given here.

**Lemma 5.1.** *[11, Lemma 6] Let $A$ be a compact convex subset of $\mathbb{R}^2$ with non-empty interior. For each point $p \in int(A)$ and $b \in \partial A$, the ray going from $p$ to $b$ only intersects $\partial A$ at $b$ (See[6] Figure 8(a).)*

[6]The Images in Figure 8 were created by L. E. Miller [18] and are used, here, with permission.

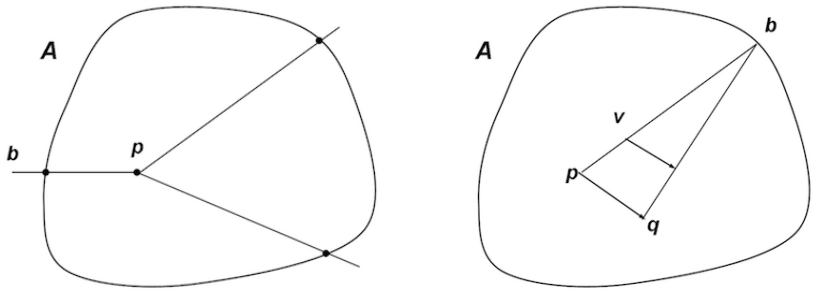


(a) Rays outward (b) Variant of a push

Figure 8: A convex set and a map defined on it

**Lemma 5.2.** *[11, Lemma 7] Let $A$ be a compact convex subset of $\mathbb{R}^2$ with non-empty interior and fix $p \in int(A)$. For each boundary point $b \in \partial A$, denote by $[p, b]$ the line segment from $p$ to $b$. Then $A = \bigcup_{b\in\partial A}[p, b]$.*

**Lemma 5.3.** *There is an ambient isotropy between $L$ and $C$ with compact support of $\Gamma$, leaving $\partial\Gamma$ fixed.*

**Proof:** We consider each normal disc $D_r(t)$ for $t \in [0, 1]$. Let $p = D_r(t) \cap C$ and $q = h(p)$ with $h$ defined by Equation 3, then define a map $F_{p,q} : D_r(t) \to D_r(t)$ such that it sends each line segment $[p, b]$ for $b \in \partial D_r(t)$, linearly onto the line segment $[q, b]$ as Figure 8(b) shows. The two previous lemmas (Lemma 5.1 and Lemma 5.2), will yield that $F_{p,q}$ is a homeomorphism, leaving $\partial D_r(t)$ fixed [18, Lemma 4.4.6].

In order to extend $F_{p,q}$ to an ambient isotopy, define $H : D_r(t) \times [0, 1] \to D_r(t)$ [18, Corollary 4.4.7] by

$$H(v, s) = \begin{cases} (1 - s)p + sq & \text{if } v = p \\ F_{p,(1-s)p+sq}(v) & \text{if } v \neq p, \end{cases}$$

where $F_{p,(1-s)p+sq}$ is a map on $D_r(t)$ analogous to $F_{p,q}$, sending each line segment $[p, b]$ for $b \in \partial D_r(t)$, linearly onto the line segment $[(1 - s)p + sq, b]$.

It is a routine [18, Corollary 4.4.7] to verify that $H(v, s)$ is well defined on the compact set $D_r(t)$, continuous, one-to-one and onto, leaving $\partial D_r(t)$ fixed. Now, we naturally define an ambient isotopy $T_t : \mathbb{R}^2 \times [0, 1] \to \mathbb{R}^2$ on the plane containing $D_r(t)$ by

$$T_t(v, s) = \begin{cases} H(v, s) & \text{if } v \in D_r(t) \\ v & \text{otherwise.} \end{cases}$$

We then define $T : \mathbb{R}^3 \times [0,1] \to \mathbb{R}^3$ by

$$T(v,s) = \begin{cases} T_t(v,s) & \text{if } v \in D_r(t) \\ v & \text{otherwise.} \end{cases}$$

The fact that the normal discs $D_r(t)$ are disjoint ensures that $T$ is an ambient isotopy [18, Corollary 4.4.8], with compact support of $\Gamma$, leaving $\partial\Gamma$ fixed. □

Now we apply this result to a simple, regular, composite, $C^1$ Bézier curve $\mathcal{B}$ and the control polygon $\mathcal{P}$. As discussed previously, there exists a nonsingular pipe surface [17] of radius $r$ for $\mathcal{B}$, denoted as $S_{\mathcal{B}}(r)$. Denote the nonsingular pipe section determined by $S_{\mathcal{B}}(r)$ as $\Gamma_{\mathcal{B}}$. Also, for each subcontrol polygon of $\mathcal{B}$, there exists a corresponding nonsingular pipe sections. Denote the nonsingular pipe section corresponding to the $k$th control polygon as $\Gamma_k$.

**Theorem 5.1.** *Each sub-control polygon $P^k$ of a Bézier curve $\mathcal{B}$ will eventually satisfy Hypotheses 1* and *2 via subdivision, and consequently, there will be an ambient isotropy between $\mathcal{B}$ and $\mathcal{P}$ with compact support of $\Gamma_{\mathcal{B}}$, leaving $\partial\Gamma_{\mathcal{B}}$ fixed.*

**Proof:** By Lemma 4.1, *Hypotheses 1* and *2* can be achieved by subdivisions. Now consider each sub-control polygon $P^k$ satisfying *Hypotheses 1* and *2*, and the corresponding Bézier sub-curves $B^k$. Use Lemma 5.3 to define an ambient isotopy $\Psi_k : \mathbb{R}^3 \times [0,1] \to \mathbb{R}^3$ between $B^k$ and $P^k$, for each $k \in \{1, 2, \ldots, 2^i\}$. Define $\Psi : \mathbb{R}^3 \times [0,1] \to \mathbb{R}^3$ by the composition

$$\Psi = \Psi_1 \circ \Psi_2 \circ \ldots \circ \Psi_{2^i}.$$

Note that $\Psi_k$ fixes the complement of $\text{int}(\Gamma_k)$, and $\text{int}(\Gamma_k) \cap \text{int}(\Gamma_{k'}) = \emptyset$ for all $k \neq k'$. So the composition $\Psi$ is well defined. Since each $\Psi_k$ is an ambient isotopy, the composition $\Psi$ is an ambient isotopy between $\mathcal{B}$ and $\mathcal{P}$ with compact support of $\Gamma_{\mathcal{B}}$, leaving $\partial\Gamma_{\mathcal{B}}$ fixed. □

## 6. Sufficient subdivision iterations for ambient isotopies

Now we consider sufficient numbers of subdivision iterations to achieve the ambient isotopy defined by Theorem 5.1. By Theorem 5.1, we shall have a control polygon that satisfies *Hypotheses 1* and *2*. The number of

subdivisions for *Hypothesis 1* is given in the companion paper [15, Lemma 6.3]. To obtain the number of subdivisions for *Hypothesis 2*, we consider the following lemmas, for which we let $\mathcal{P}'(t) = l'(P, i)(t)$ (the first derivative of the control polygon $\mathcal{P}$), and denote the angle between $\mathcal{B}'(t)$ and $\mathcal{P}'(t)$ as $\theta(t)$, for $t \in [0, 1]$.

**Lemma 6.1.** *For any $0 < \nu < \frac{\pi}{2}$, let $N(\nu)$ be the value given in the companion paper* [15, Equation 20]*, then after $N(\nu)$ subdivisions, we have $\max_{t\in[0,1]} \theta(t) < \nu$.*

**Proof:** Note (similarly as [15, Inequality 6])

$$1 - \cos(\theta(t)) = 1 - \frac{\mathcal{B}'(t) \cdot \mathcal{P}'(t)}{||\mathcal{B}'(t)|| \cdot ||\mathcal{P}'(t)||}$$

$$= \frac{||\mathcal{B}'(t)|| \cdot ||\mathcal{P}'(t)|| - \mathcal{P}'(t) \cdot \mathcal{P}'(t) + \mathcal{P}'(t) \cdot \mathcal{P}'(t) - \mathcal{B}'(t) \cdot \mathcal{P}'(t)}{||\mathcal{B}'(t)|| \cdot ||\mathcal{P}'(t)||}$$

$$\leq \frac{||\mathcal{B}'(t)|| - ||\mathcal{P}'(t)||}{||\mathcal{B}'(t)||} + \frac{||\mathcal{B}'(t) - \mathcal{P}'(t)||}{||\mathcal{B}'(t)||} \leq \frac{2||\mathcal{B}'(t) - \mathcal{P}'(t)||}{\sigma},$$

where $\sigma = \min\{||\mathcal{B}'(t)|| : t \in [0, 1]\}$ (Recall $\sigma > 0$.) From the companion paper [15, Inequality 12]

$$\max_{t\in[0,1]} ||\mathcal{B}'(t) - \mathcal{P}'(t)|| \leq B'_{dist}(i),$$

we have

$$1 - \cos(\theta(t)) \leq \frac{2B'_{dist}(i)}{\sigma}.$$

Then from the companion paper [15, Inequality 16] (Note that this inequality is valid for $i > N(\nu)$)

$$\frac{2(2B'_{dist}(i) + \gamma/(n2^i))}{\sigma - B'_{dist}(N_1)} < 1 - \cos(\nu),$$

we get

$$1 - \cos(\theta(t)) \leq \frac{2B'_{dist}(i)}{\sigma} < \frac{2(2B'_{dist}(i) + \gamma/(n2^i))}{\sigma - B'_{dist}(N_1)} < 1 - \cos(\nu).$$

So $\cos(\theta(t)) > \cos(\nu)$. Note that $\theta(t)$ is an exterior angle with measure between 0 and $\pi$ and $0 < \nu < \frac{\pi}{2}$ by the hypothesis. Since $\cos x$ is monotonically decreasing when $x \in [0, \frac{\pi}{2}]$, we have $\theta(t) < \nu$. This is true for all $t \in [0, 1]$, so $\max_{t\in[0,1]} \theta(t) < \nu$. □

**Lemma 6.2.** *Performing $N(\frac{\pi}{2n})$ subdivisions will yield a control polygon $\mathcal{P}$ with each sub-control $P^k$ satisfying Hypothesis 2:*

$$T_\kappa(P^k) + \max_{t\in[0,1]} \theta(t) < \frac{\pi}{2}.$$

**Proof:** Recall that $N(\frac{\pi}{2n})$ given in the companion paper [15, Equation 20] is a sufficient number of subdivisions to produce $\mathcal{P}$ such that all exterior angles are less than $\frac{\pi}{2n}$, as shown in the companion paper [15, Theorem 6.1]. Note that each $P^k$ has $n-1$ exterior angles. So after $N(\frac{\pi}{2n})$ subdivisions, we have

$$T_\kappa(P^k) < \frac{\pi(n-1)}{2n}.$$

By Lemma 6.1, after $N(\frac{\pi}{2n})$ subdivisions, we also have

$$\max_{t\in[0,1]} \theta(t) < \frac{\pi}{2n}.$$

So, after $N(\frac{\pi}{2n})$ subdivisions, we obtain

$$T_\kappa(P^k) + \max_{t\in[0,1]} \theta(t) < \frac{\pi(n-1)}{2n} + \frac{\pi}{2n} = \frac{\pi}{2}.$$

□

Let

$$N^\star = \max\{N(\frac{\pi}{2n}), N'(r)\}, \tag{13}$$

where $r$ is the radius of $S_r(\mathcal{B})$.

**Theorem 6.1.** *Performing $N^\star$ or more subdivisions, where $N^\star$ is given by Equation 13, will produce an ambient isotopic $\mathcal{P}$ for $\mathcal{B}$.*

**Proof:** According to the companion paper [15, Lemma 6.3], *Hypothesis 1* is satisfied after $N'(r)$ subdivisions. By Lemma 6.2, *Hypothesis 2* is satisfied after $N(\frac{\pi}{2n})$ subdivisions. Then Theorem 5.1 can be applied to draw the conclusion. □

*Hypothesis 2* is motivated by the weaker condition $T_\kappa(P^k) < \frac{\pi}{2}$. We couldn't derive the same results by using this weaker condition instead, but our *Hypothesis 2* requires at most one more subdivision, as shown below.

**Remark 6.1.** *The sufficient number of subdivisions for Hypothesis 2 is at most one more than that for the weaker condition* $T_\kappa(P^k) < \frac{\pi}{2}$.

**Proof:** By the above proof of Lemma 6.2 we know that $N(\frac{\pi}{2(n-1)})$ subdivisions are sufficient to guarantee $T_\kappa(P^k) < \frac{\pi}{2}$, while $N(\frac{\pi}{2n})$ subdivisions are sufficient to obtain $T_\kappa(P^k) + \max_{t\in[0,1]} \theta(t) < \frac{\pi}{2}$. The function $N(\cdot)$ is given in the companion paper [15, Equation 20], that is,

$$N(\nu) = \max\{N_1, N_2, \log(f(\nu))\},$$

where $N_1$ and $N_2$ are constants for a given $\mathcal{B}$, and the function $f(\cdot)$ is defined in the companion paper [15, Equation 19]:

$$f(\nu) = \frac{c_{\mathcal{B}}}{1-\cos\nu},$$

where $c_{\mathcal{B}}$ is a constant. Note that,

$$N(\frac{\pi}{2(n-1)}) = \max\{N_1, N_2, \log(f(\frac{\pi}{2(n-1)}))\}$$

and

$$N(\frac{\pi}{2n}) = \max\{N_1, N_2, \log(f(\frac{\pi}{2n}))\}.$$

So comparing $N(\frac{\pi}{2(n-1)})$ with $N(\frac{\pi}{2n})$ is essentially comparing $\log(f(\frac{\pi}{2(n-1)}))$ with $\log(f(\frac{\pi}{2n}))$. So we consider

$$\log(f(\frac{\pi}{2n})) - \log(f(\frac{\pi}{2(n-1)})) = \log\frac{f(\frac{\pi}{2n})}{f(\frac{\pi}{2(n-1)})} = \log\frac{1-\cos(\frac{\pi}{2(n-1)})}{1-\cos(\frac{\pi}{2n})}.$$

As before, we consider only $n \geq 3$, since for $\mathcal{B}$ of degree 1 or 2, the control polygon is trivially simple and ambient isotopic to $\mathcal{B}$, provided the regularity of $\mathcal{B}$.

Consider the expression inside the logarithm as a function of $x$:

$$\frac{1-\cos(\frac{\pi}{2(x-1)})}{1-\cos(\frac{\pi}{2x})}.$$

Since its derivative is negative for $x \geq 3$, we have that

$$\log(f(\frac{\pi}{2n})) - \log(f(\frac{\pi}{2(n-1)})) \leq \log\frac{1-\cos(\frac{\pi}{2(3-1)})}{1-\cos(\frac{\pi}{2\cdot 3})} \approx 0.78.$$

This implies that

$$N(\frac{\pi}{2n}) - N(\frac{\pi}{2(n-1)}) < 1,$$

for any $n \geq 3$. □

## 7. Conclusion

We showed that sufficiently many subdivisions produce a control polygon ambient isotopic to a given Bézier curve $\mathcal{B}$. We established closed-form formulas to compute *a priori* sufficient number of subdivisions to achieve the isotopy. The proof here is based on explicitly constructing homeomorphisms and ambient isotopies, which is motivated by the goal of minimizing subdivision iterations for practical applications. In contrast, the pure existence proof [12] requires the convex hulls of sub-control polygons to be contained in the tubular neighborhood determined by a pipe surface and may need more subdivision iterations and produce too many $PL$ segments. This method here has another theoretical consequence: we established two criteria (*Hypotheses 1, 2*) to ensure the ambient isotopy between a $PL$ curve and a $C^2$ curve connected at the end points.

These results have potential applications in computer graphics, computer animation and scientific visualization, especially in visualizing molecular simulations.

## References


[1] N. Amenta, T. J. Peters, and A. C. Russell. Computational topology: Ambient isotopic approximation of 2-manifolds. *Theoretical Computer Science*, 305:3–15, 2003.

[2] L. E. Andersson, S. M. Dorney, T. J. Peters, and N. F. Stewart. Polyhedral perturbations that preserve topological form. *CAGD*, 12(8):785–799, 2000.

[3] J. Bisceglio, T. J. Peters, J. A. Roulier, and C. H. Sequin. Unknots with highly knotted control polygons. *CAGD*, 28(3):212–214, 2011.

[4] M. Burr, S. W. Choi, B. Galehouse, and C. K. Yap. Complete subdivision algorithms, II: Isotopic meshing of singular algebraic curves. *Journal of Symbolic Computation*, 47:131–152, 2012.

[5] Frédéric Chazal, David Cohen-Steiner, and Quentin Mérigot. Geometric inference for probability measures. *Foundations of Computational Mathematics*, 11:733–751, 2011.

[6] W. Cho, T. Maekawa, and N. M. Patrikalakis. Topologically reliable approximation in terms of homeomorphism of composite Bézier curves. *Computer Aided Geometric Design*, 13:497–520, 1996.

[7] E. Denne and J. M. Sullivan. Convergence and isotopy type for graphs of finite total curvature. *Discrete Differential Geometry*, 38(Part II):163–174, 2008.

[8] M. P. do Carmo. *Differential Geometry of Curves and Surfaces*. Prentice Hall, Upper Saddle River, NJ, 1976.

[9] G. Farin. *Curves and Surfaces for Computer Aided Geometric Design*. Academic Press, San Diego, CA, 1990.

[10] M. W. Hirsch. *Differential Topology*. Springer, New York, 1976.

[11] K. E. Jordan, L. E. Miller, T. J. Peters, and A. C. Russell. Geometric topology and visualizing 1-manifolds. In V. Pascucci, X. Tricoche, H. Hagen, and J. Tierny, editors, *Topological Methods in Data Analysis and Visualization*, pages 1 – 13. Springer NY, 2011.

[12] J. Li. *Topological and Isotopic Equivalence with Applications to Visualization*. PhD thesis, University of Connecticut, U.S., 2013 expected.

[13] J. Li and T. J. Peters. Isotopy convergence theorem. *Preprint*, 2012.

[14] J. Li, T. J. Peters, D. Marsh, and K. E. Jordan. Computational topology counterexamples with 3D visualization of Bézier curves. *Applied General Topology*, 2012.

[15] J. Li, T. J. Peters, and J. A. Roulier. Topology during subdivision of Bézier curves I: Angular convergence & homeomorphism. *Preprint*, 2012.

[16] L. Lin and C. Yap. Adaptive isotopic approximation of nonsingular curves: the parameterizability and nonlocal isotopy approach. *Discrete & Computational Geometry*, 45 (4):760–795, 2011.

[17] T. Maekawa, N. M. Patrikalakis, T. Sakkalis, and G. Yu. Analysis and applications of pipe surfaces. *CAGD*, 15(5):437–458, 1998.

[18] L. E. Miller. *Discrepancy and Isotopy for Manifold Approximations*. PhD thesis, University of Connecticut, U.S., 2009.

[19] J. W. Milnor. On the total curvature of knots. *Annals of Mathematics*, 52:248–257, 1950.

[20] G. Monge. *Application de l'Analys à la Geometrie*. Bachelier, Paris, 1850.

[21] E. L. F. Moore. *Computational Topology of Spline Curves for Geometric and Molecular Approximations*. PhD thesis, University of Connecticut, U.S., 2006.

[22] E. L. F. Moore, T. J. Peters, and J. A. Roulier. Preserving computational topology by subdivision of quadratic and cubic Bézier curves. *Computing*, 79(2-4):317–323, 2007.

[23] G. Morin and R. Goldman. On the smooth convergence of subdivision and degree elevation for Bézier curves. *CAGD*, 18:657–666, 2001.

[24] J. Munkres. *Topology*. Prentice Hall, 2nd edition, 1999.

[25] D. Nairn, J. Peters, and D. Lutterkort. Sharp, quantitative bounds on the distance between a polynomial piece and its Bézier control polygon. *CAGD*, 16:613–631, 1999.

[26] M. Neagu, E. Calcoen, and B. Lacolle. Bézier curves: Topological convergence of the control polygon. *6th Int. Conf. on Mathematical Methods for Curves and Surfaces, Vanderbilt*, pages 347–354, 2000.

[27] M. Reid and B. Szendroi. *Geometry and Topology*. Cambridge University Press, 2005.